The 17th International Electronic Conference on Synthetic Organic Chemistry

SYNTHESIS OF A NOVEL FAMILY OF PORPHYRIN WITH TRIPHENYLAMINE DONOR GROUPS TO BE APPLIED IN DYE SENSITIZED SOLAR CELLS

Ana Aljarilla,[a] John N. Clifford,[*b] Laia Pellejà,[b] Antonio Moncho,[b] Susana Arrechea,[a] Pilar de la Cruz,[a] Fernando Langa[*a] and Emilio Palomares[bc]

[a]*Institute of Nanoscience, Nanotechnology and Molecular Materials (INAMOL), Campus de la Fábrica de Armas (UCLM), Toledo, Spain. E-mail: Fernando.Langa@uclm.es; Fax: 34 9252 68840; Tel: 34 9252 68843;*

[b]*Institute of Chemical Research of Catalonia (ICIQ), Avda. Països Catalans 16, Tarragona E-43007, Spain. E-mail: jnclifford@iciq.es; Fax: +34 9779 20224; Tel: +34 9779 20200.*

[c]*ICREA, Avda. Lluís Companys 28, Barcelona E-08030, Spain.*

ABSTRACT

The solar cells of third generation, which can be classified in hybrids and organics, are the target of uncountable studies and developments along the last few years. These cells present low fabrication cost, flexibility, lightness, and stability. In this work two new Zinc–porphyrin **1a** and **1b**, bearing triphenylamine donor groups were synthesized and their efficiencies measured in nanocrystalline TiO_2 dye sensitized solar cells employing iodide/tri-iodide and tris(1,10-phenanthroline) cobalt electrolytes. Optimized sensitization time for the TiO_2 photoanode was found to depend on the electrolyte employed: devices based on iodide/tri-iodide showed better efficiencies with shorter sensitization times (1.5 hours) whereas those based on tris(1,10-phenanthroline) cobalt showed better efficiencies with longer sensitization times (6 hours). From UV-Vis absorption spectra it is estimated that there is roughly twice as much dye loaded onto the TiO_2 film sensitized for 6 hours compared to the 1.5 hour film.

KEYWORDS: porphyrin, photovoltaics, dyes, sensitizer

INTRODUCTION

Research into Dye Sensitized Solar Cells (DSCs) continues to be an extremely active area.[1-4] After considerable time in which DSCs based on Ru(II) polypyridyl sensitizers were clearly the most efficient, DSCs based on fully organic sensitizers have recently made huge strides forward in development.[5,6] In particular, there are many recent examples of DSC devices employing iodide/tri-iodide (I^-/I_3^-) with >10% device efficiency based on D-π-A porphyrins designed by Diau and co-workers.[7-9] Indeed, with recently developed novel cobalt based complexes [10-13] porphyrins have shown their promise with the current highest efficiency recorded for a DSC device of 12.05% being based on a cell containing a porphyrin sensitizer and a tris(bipyridyl) cobalt electrolyte.[12] Regardless of the red/ox couple, porphyrins offer several distinct advantages over Ru(II)polypyridyl sensitizers due to their high molar extinction coefficients, sharp absorption bands and high photostability.[15,17]

Full research published in Journal of Materials Chemistry A, on September 25th, 2013. Cite this: DOI: 10.1039/c3ta12955a

However, their properties in DSCs still need to be fully investigated and molecular structure-device function rules need to be outlined to fully understand device performance for devices based on these dyes.

We investigate the performance of two porphyrin sensitizers, **1a** and **1b** (Scheme 1), in DSC devices employing I^-/I_3^- and tris(1, 10-phenanthroline) cobalt electrolytes.

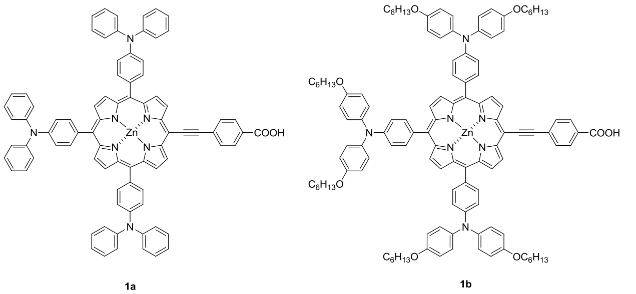

Scheme 1 Structures of dyes **1a** and **1b**.

RESULTS AND DISCUSSION

Synthesis of 1a and 1b

Scheme 2 illustrates the synthetic route to dyes **1a** and **1b**. We prepared the free base porphyrins **2a,b** in 14% and 11% yield respectively, according to the Lindsey method.[18] This procedure improves significantly the yield with respect to previous procedures described for similar porphyrins (4-6%).[19] **2a,b** were reacted with zinc acetate in chloroform giving the metallated porphyrins **3a,b** in 91% and 95% yield after purification by column chromatography (silica gel, Hex/$CHCl_3$, 1:1). Finally, the trimethylsylil group was quantitatively removed by TBAF and *in situ* reacted with *p*-iodobenzoic acid under Pd-catalyzed Sonogashira coupling conditions affording the target dyes **1a,b** in 70 and 63% yield respectively. The intermediate and final compounds were fully characterized by means of UV-Vis, FT-IR, ^1H and ^{13}C NMR spectroscopies; the structures of all compounds were confirmed by MALDI-TOF mass spectrometry.

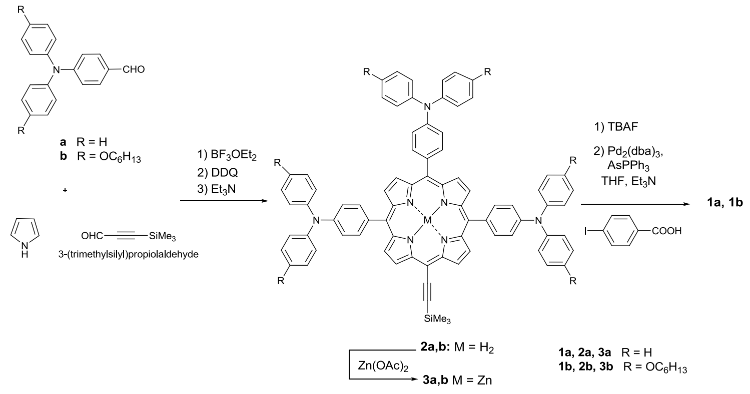

Scheme 2 Synthetic route to dyes **1a** and **1b**.

The thermal stabilities of compounds **1a** and **1b** were evaluated by thermogravimetric analysis (TGA) under nitrogen, with a heating rate of 10 ºC/min. The decomposition temperatures (Td) were estimated from the TGA plot as the temperature of the intercept of the leading edge of the weight loss curve. Under these conditions, compounds **1a** and **1b** display excellent thermal stability up to 220 ^{o}C which are in principle satisfactory for application in photovoltaic devices.

Absorption, emission, electrochemistry and computational calculations

The absorption spectra of dyes **1a,b** in dichloromethane (CH_2Cl_2) solution are shown in Fig. 1. Both dyes exhibit the typical features of zinc porphyrins, with an intense Soret band between 400-500 nm and less intense Q bands in the range 550 to 700 nm (see Table 1). As expected, the absorption bands are not very sensitive to the nature of the substituents, pointing to weak electronic interactions between the porphyrin and the attached moiety in the ground state. Due to the presence of the hexyloxy groups in dye **1b**, a bathochromic shift is observed in the Q band, while in the Soret band an enhancement in bandwidth is observed. For the fluorescence spectra in CH_2Cl_2 the trend for the variation of the emission wavelength is similar to that of the absorption bands. The emission bands at 652 nm (**1a**, λ_{exc}= 450 nm) and 669 nm (**1b**, λ_{exc}= 449 nm) (Fig. 1) were totally quenched after adsorption onto TiO_2 indicating efficient photoinduced electron transfer from the dyes to the TiO_2 nanoparticles.

The redox properties of **1a,b** were investigated by cyclic voltammetry and square wave voltammetry in tetrahydrofurane (THF). In the cathodic side, compounds **1a,b** show the first reversible oxidation peaks at 0.33 and 0.28 V respectively; the presence of the electron-donating alkoxy groups significantly reduces the oxidation potential of **1b** compared to **1a**. On the reduction side, both compounds show first reduction potentials at -0.52 V and -0.57 V as irreversible waves, showing that the electron-donating alkoxy groups in **1b** increase its reduction potential with respect to **1a**, as one would expect. The E_{HOMO} values of **1a** to **1b** vary only by 0.05 eV and were determined as -5.43 eV (**1a**) and -5.38 eV (**1b**), indicating regeneration is energetically feasible by I/I_3^- (E_{redox} = -4.75 eV) and $Co(II)(phen)_3/Co(III)(phen)_3$ (E_{redox} = -5.06 eV) red/ox couples. The E_{LUMO} values also indicate that efficient electron injection into the TiO_2 conduction band (E_{TiO2} = -4.00 eV) is also energetically possible.

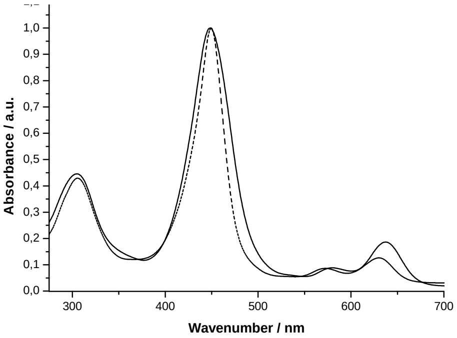

Fig. 1 Normalized absorption spectra of dyes **1a** (--) and **1b** (–) in dichloromethane solution (10^{-5} M).

Full research published in Journal of Materials Chemistry A, on September 25th, 2013. Cite this: DOI: 10.1039/c3ta12955a

Table 1 Absorption, emission and electrochemical data of dyes **1a** and **1b**.

	$\lambda_{max}{}^{a}$/nm (log ε)	$\lambda_{em}{}^{a}$/ nm	$E^{1}{}_{red}{}^{b}$ (V)	$E^{1}{}_{ox}{}^{b}$(V)	$E_{HOMO}{}^{c}$ (eV)	$E_{LUMO}{}^{d}$ (eV)
1a	630 (4.18), 572 (4.02), 450 (5.08), 306 (4.71)	652	-0.52	0.33	-5.43	-3.50
1b	637 (4.39), 579 (4.07), 449 (5.12), 305 (4.77)	669	-0.58	0.28	-5.38	-3.49

[a] 10^{-5} M, CH_2Cl_2. [b] [10^{-3} M] in THF versus Fc/Fc+, glassy carbon, Pt counter electrode, 20 ºC, 0.1 M Bu_4NClO_4, scan rate = 100 mV s^{-1}. [c] Calculated using equation E_{LUMO} (vs. vacuum) = -5.1 - $E^{1}{}_{ox}$ (vs. Fc/Fc+) in eV.[20] [d] E_{LUMO} was calculated using $E_{LUMO} = E_{HOMO} + E_{0\text{-}0}$, where $E_{0\text{-}0}$ is the intersection of the absorption and emission spectra.

In order to gain insight into the geometries and electronic properties of dyes **1a** and **1b**, computational studies were performed using density functional theory (DFT) at the B3LYP/6-31G level. Regarding geometry, for both dyes the dihedral angles between the phenyl ring and the porphyrin macrocycle (φ) are similar ($\varphi \sim$ -65º) and are in agreement with those calculated for similar systems (Fig. 2).[21] The HOMOs were found to be delocalized through both the porphyrin macrocycle and TPA for both **1a** and **1b**, whereas the LUMOs are extended along the porphyrin system, the linker and the acid group, indicating electronic coupling with the TiO_2 nanocrystals. The HOMO-LUMO gap is similar for both dyes although the LUMO level of dye **1b** is higher (-2.45 eV) than that of **1a** (-2.61 eV) due to the electronic coupling of the alkoxy groups of the TPA moieties. HOMO and LUMO (Fig. 3) are overlapped, favouring the HOMO to LUMO electronic transitions.

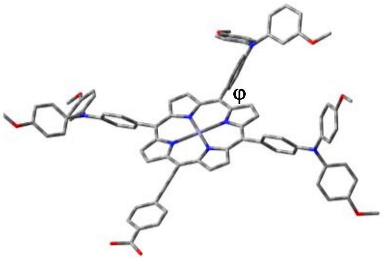

Fig. 2 Optimized structure for dye **1b** (hexyl groups have been changed by methyl for calculations).

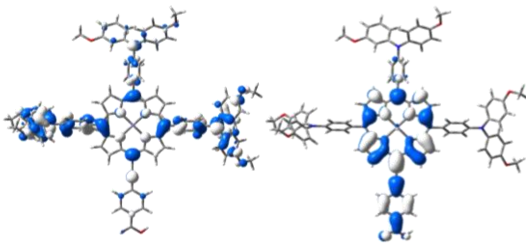

Fig. 3 Frontier orbitals of dye **1b:** HOMO (left) and LUMO (right).

Device properties

Fig. 4 and Table 2 show the IV curves and device characteristics, namely J_{sc}, V_{oc}, fill factor (*FF*) and overall efficiency (η), for sensitizers **1a** and **1b** in DSC devices based on I^-/I_3^- and Co(II)(phen)$_3$/Co(III)(phen)$_3$ electrolytes.

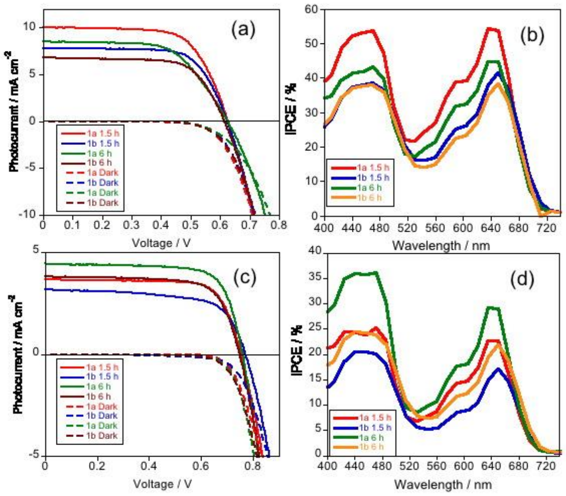

Fig. 4 *I*-*V* curves and IPCE spectra of DSC devices composed of sensitizers **1a** and **1b** based on I^-/I_3^- ((a) and (b)) and Co(II)(phen)$_3$/Co(III)(phen)$_3$ electrolytes ((c) and (d)).

Table 2 Photovoltaic performance of cells recorded under AM 1.5G 1 sun illumination.

Dye	Time	J_{sc} (mA/cm^2)	V_{oc} (V)	*FF* (%)	η ^{d} (%)
1a	1.5 hours^a	10.09	0.63	67	4.19 (5.14)
1a	6 h^a	8.51	0.62	62	3.27 (3.93)
1b	1.5 hours^a	7.83	0.62	70	3.40 (4.15)
1b	6 h^a	6.18	0.61	69	2.54 (3.60)
1a	1.5 hours^b	3.67	0.75	75	2.06 (2.53)
1a	6 h. ^{b}	4.44	0.76	74	2.48 (3.11)
1b	1.5 hours^b	3.17	0.77	66	1.61 (2.01)
1b	6 h ^{b}	3.82	0.75	72	2.05 (2.45)
YD2-o-C8^c		15.25	0.76	72	8.42 (11.20)

[a] Electrolyte: 0.6 M 1-butyl-3-methylimidazolium iodide (BMII), 0.1 M lithium iodide, 0.05 M iodine and 0.5 M 4-*tert*-butylpyridine in a 1:1 mixture of acetonitrile-valeronitrile. [b]Electrolyte: 0.2 M tris(1,10-phenanthroline)cobalt(II)(TFSI)$_2$, 0.02 M tris(1,10-phenanthroline) cobalt(III)(TFSI)$_3$, 0.1 M lithium perchlorate and 0.5 M 4-*tert*-butylpyridine in a 85:15 mixture of acetonitrile-valeronitrile. [c]Electrolyte: 0.5 M 1-butyl-3-methylimidazolium iodide (BMII), 0.05 M lithium iodide, 0.05 M iodine, and 0.5 M 4-tert-butylpyridine in a 85:15 mixture of acetonitrile-valeronitrile. *Data in parenthesis recorded without mask.

Employing I^-/I_3^- electrolyte, the best device efficiencies (Fig. 4(a)) were obtained after 1.5 hours sensitization time with maximum efficiencies of 5.14% and 4.15% for **1a** and **1b** respectively (without mask). These values compare well with a recent study by Liu *et al.* involving similar dyes.[19]

Upon the longer sensitization time of 6 hours the device efficiency drops to 3.93% and 3.60% for **1a** and **1b** respectively (without mask). The principle reason for this is a loss in J_{sc}. When cobalt electrolyte is used, however, the dependence of device efficiency on sensitization time is reversed (Fig. 4(c)). The best efficiencies are recorded for 6 hours sensitization (3.11% and 2.45% for **1a** and **1b** respectively). Again, the main difference appears to be accounted for by a difference in J_{sc}. The increase in device V_{oc} (approx. 140 mV) afforded by employing $Co(II)(phen)_3/Co(III)(phen)_3$ with respect to I^-/I_3^- is in line with that observed in other studies.[22] Finally, under similar conditions the **YD2-o-C8** device gave an efficiency of 11.20% (without mask) indicating testing conditions are indeed comparable with studies demonstrating the best literature values for porphyrin based DSCs.[23] Fig. 4(b) and (d) show the IPCE spectra for all of the devices measured in this study. These spectra show the contributions to device current from the Soret and Q bands centred at around 450 and 650nm respectively. Integration of these spectra agrees with the J_{sc} values for the same devices in Fig. 4(a) and (c).

In order to have an indication of dye loading in these devices, the absorption spectra of thin films of transparent TiO_2 films (6 µm) were measured after 1.5 hours and 6 hour sensitization in 0.2 mM solutions of **Ia** and **Ib** in chlorobenzene (Fig. 5). These data indicate that there is roughly twice as much dye loading on the films for 6 hours compared to the equivalent film of 1.5 hours.

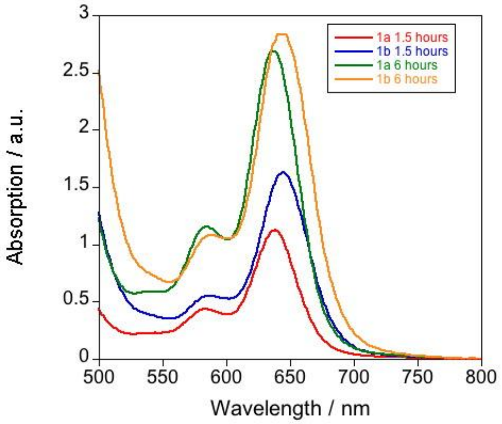

Fig. 5 Absorption spectra of thin films of transparent TiO_2 films (6 µm) following 1.5 and 6 hour sensitization in 0.2 mM solutions of **Ia** and **Ib** in chlorobenzene.

CONCLUSIONS

Two zinc-porphyrin sensitizers were synthesized and their efficiencies measured in dye sensitized solar cells employing I^-/I_3^- and $Co(II)(phen)_3/Co(III)(phen)_3$ electrolytes. Optimized sensitization times were found to depend on the electrolyte used with devices based on I^-/I_3^- showing better efficiencies with shorter sensitization times (1.5 hours) while those based on $Co(II)(phen)_3/Co(III)(phen)_3$ showing better efficiencies with longer sensitization times (6 hours). UV-Vis absorption spectra indicate that there is roughly twice as much dye loaded onto the TiO_2 film sensitized for 6 hours. This work demonstrates how device preparation must be tailored carefully depending on the electrolyte red/ox couple used.

ACKNOWLEDGEMENTS

Financial support from the Ministry of Science and Innovation of Spain, (CTQ2010-17498, PLE2009-0038 and Consolider- Ingenio Projects HOPE CSD2007-00007) is gratefully acknowledged. EP would also like to thank the EU for the ERCstg PolyDot, and the Catalan government for the 2009 SGR-207 projects.

NOTES AND REFERENCES

1. B. O'Regan and M. Gratzel, Nature, 1991, 353, 737–740.
2. Hagfeldt, G. Boschloo, L. Sun, L. Kloo and H. Pettersson, Chem. Rev., 2010, 110, 6595–6663.
3. J. N. Clifford, E. Martinez-Ferrero and E. Palomares, J. Mater. Chem., 2012, 22, 12415–12422.
4. N. Robertson, Angew. Chem., Int. Ed., 2008, 47, 1012–1014.
5. J. N. Clifford, M. Planells and E. Palomares, J. Mater. Chem., 2012, 22, 24195–24201.
6. Mishra, M. K. R. Fischer and P. B¨auerle, Angew. Chem., Int. Ed., 2009, 48, 2474–2499.
7. T. Bessho, S. M. Zakeeruddin, C.-Y. Yeh, E. W.-G. Diau and M. Gr¨atzel, Angew. Chem., Int. Ed., 2010, 49, 6646–6649.
8. Y.-C. Chang, C.-L. Wang, T.-Y. Pan, S.-H. Hong, C.-M. Lan, H.-H. Kuo, C.-F. Lo, H.-Y. Hsu, C.-Y. Lin and E. W.-G. Diau, Chem. Commun., 2011, 47, 8910–8912.
9. C.-L. Wang, Y.-C. Chang, C.-M. Lan, C.-F. Lo, E. Wei-Guang Diau and C.-Y. Lin, Energy Environ. Sci., 2011, 4, 1788–1795.
10. S. M. Feldt, E. A. Gibson, E. Gabrielsson, L. Sun, G. Boschloo and A. Hagfeldt, J. Am. Chem. Soc., 2010, 132, 16714–16724.
11. M. Wang, C. Gratzel, S. M. Zakeeruddin and M. Gratzel, Energy Environ. Sci., 2012, 5, 9394–9405.
12. J. Cong, X. Yang, L. Kloo and L. Sun, Energy Environ. Sci., 2012, 5, 9180–9194.
13. E. Mosconi, J.-H. Yum, F. Kessler, C. J. Gomez-Garcia, C. Zuccaccia, A. Cinti, M. K. Nazeeruddin, M. Graetzel and F. De Angelis, J. Am. Chem. Soc., 2012, 134, 19438–19453.
14. Yella, H. W. Lee, H. N. Tsao, C. Y. Yi, A. K. Chandiran, M. K. Nazeeruddin, E. W. G. Diau, C. Y. Yeh,
15. S. M. Zakeeruddin and M. Gratzel, Science, 2011, 334, 629–634.
16. L. L. Li and E. W. G. Diau, Chem. Soc. Rev., 2013, 42, 291–304.
17. H. Imahori, S. Hayashi, H. Hayashi, A. Oguro, S. Eu, T. Umeyama and Y. Matano, J. Phys. Chem. C, 2009, 113, 18406–18413. M. V. Martinez-Diaz, G. de la Torre and T. Torres, Chem. Commun., 2010, 46, 7090–7108.
18. J. S. Lindsey, S. Prathapan, T. E. Johnson and R. W. Wagner, Tetrahedron, 1994, 50, 8941–8968.
19. B. Liu, W. Zhu, Y. Wang, W. Wu, X. Li, B. Chen, Y.-T. Long and Y. Xie, J. Mater. Chem., 2012, 22, 7434–7444.
20. C. M. Cardona, W. Li, A. E. Kaifer, D. Stockdale and G. C. Bazan, Adv. Mater., 2011, 23, 2367–2371.
21. M. J. Frisch, G. W. Trucks, H. B. Schlegel, G. E. Scuseria, M. A. Robb, J. R. Cheeseman, J. A. Montgomery Jr, T. Vreven, K. N. Kudin, J. C. Burant, J. M. Millam, S. S. Iyengar, J. Tomasi, V. Barone, B. Mennucci, M. Cossi, G. Scalmani, N. Rega, G. A. Petersson, H. Nakatsuji, M. Hada, M. Ehara, K. Toyota, R. Fukuda, J. Hasegawa, M. Ishida, T. Nakajima, Y. Honda, O. Kitao, H. Nakai, M. Klene, X. Li, J. E. Knox, H. P. Hratchian, J. B. Cross, V. Bakken, C. Adamo, J. Jaramillo, R. Gomperts, R. E. Stratmann, O. Yazyev, A. J. Austin, R. Cammi, C. Pomelli, J. W. Ochterski, P. Y. Ayala, K. Morokuma, G. A. Voth, P. Salvador, J. J. Dannenberg, V. G. Zakrzewski, S. Dapprich, A. D. Daniels, M. C. Strain, O. Farkas, D. K. Malick, A. D. Rabuck, K. Raghavachari, J. B. Foresman, J. V. Ortiz, Q. Cui, A. G. Baboul, S. Clifford, J. Cioslowski, B. B. Stefanov, G. Liu, A. Liashenko, P. Piskorz, I. Komaromi, R. L. Martin, D. J. Fox, T. Keith, M. A. Al-Laham, C. Y. Peng, A. Nanayakkara, M. Challacombe, P. M.

W. Gill, B. Johnson, W. Chen, M. W. Wong, C. Gonzalez and J. A. Pople, R. D. Gaussian 03, Gaussian Inc., Wallingford CT, 2004.

22. Y. Bai, J. Zhang, D. Zhou, Y. Wang, M. Zhang and P. Wang, J. Am. Chem. Soc., 2011, 133, 11442–11445.
23. H.-P. Wu, Z.-W. Ou, T.-Y. Pan, C.-M. Lan, W.-K. Huang, H.-W. Lee, N. M. Reddy, C.-T. Chen, W.-S. Chao, C.-Y. Yeh and E. W.-G. Diau, Energy Environ. Sci., 2012, 5, 9843–9848.
24. S. E. Koops, P. R. F. Barnes, B. C. O'Regan and J. R. Durrant, J. Phys. Chem. C, 2010, 114, 8054–8061
25. S. Tatay, S. A. Haque, B. O'Regan, J. R. Durrant, W. J. H. Verhees, J. M. Kroon, A. Vidal-Ferran, P. Gavina and E. Palomares, J. Mater. Chem., 2007, 17, 3037–3044.
26. T. Zewdu, J. N. Clifford, J. P. Hernandez and E. Palomares, Energy Environ. Sci., 2011, 4, 4633–4638.
27. H.-M. Nguyen, R. S. Mane, T. Ganesh, S.-H. Han and N. Kim, J. Phys. Chem. C, 2009, 113, 9206–9209.